19th Brazilian Congress of Thermal Sciences and Engineering
November 06th-10th, 2022, Bento Gonçalves - RS - Brazil

ENC-2022-0331
EXPERIMENTAL AND NUMERICAL STUDY OF HEAT TRANSFER AND PRESSURE DROP IN MICRO PIN FIN HEAT SINKS UNDER DIFFERENT FLOW CONDITIONS

Jéssica Martha Nunes
UNESP - São Paulo State University, Campus of Ilha Solteira, Av. Brasil, 56, 15385-000, Ilha Solteira, SP, Brazil
jessica.nunes@unesp.br

Isabelle Guimarães da Silva
UNESP - São Paulo State University, Campus of São João da Boa Vista, São João da Boa Vista, SP, Brazil
isabelle.g.silva@unesp.br

João Batista Campos Silva
UNESP - São Paulo State University, Campus of Ilha Solteira, Av. Brasil, 56, 15385-000, Ilha Solteira, SP, Brazil
campos.silva@unesp.br

Jeferson Diehl de Oliveira
FSG-University Center, Department of Mechanical Engineering, Os Dezoito do Forte, 2366, Caxias do Sul 95020-472, RS, Brazil
jeferson.oliveira@fsg.edu.br

Jacqueline Biancon Copetti
UNISINOS - University of Vale do Rio dos Sinos, LETEF - Laboratory of Thermal and Fluid Dynamic Studies, São Leopoldo 93022-750, RS, Brazil
jcopetti@unisinos.br

Elaine Maria Cardoso*
UNESP - São Paulo State University, Campus of Ilha Solteira, Av. Brasil, 56, 15385-000 Ilha Solteira, SP, Brazil
UNESP - São Paulo State University, Campus of São João da Boa Vista, São João da Boa Vista, SP, Brazil
*elaine.cardoso@unesp.br

Abstract. *Due to microscale effects, the segmented microchannels or micro pin fins heat sinks came out as a high thermal management solution. In this context, the present work analyzes the influence of different heights of micro pin fins with an aligned array and investigates their influence on pressure drop and heat transfer behavior. The HFE-7100 is used as the working fluid, and the pressure drop and surface temperature behavior are analyzed for different mass fluxes and inlet subcooling. The CFD software ANSYS FLUENT® was applied for single-phase flow to compare it with the experimental data. The numerical analysis shows that the highest micro pin fins configuration provides a more uniform wall temperature distribution and decreases by around 18.6% compared to the lowest configuration. There is a good agreement between the experimental results and the numerical analysis, with a mean absolute error of 6% for all the considered parameters. For the two-phase flow condition, for the highest subcooling, an increase in mass flux causes an enhancement in the heat transfer for low heat flux; by increasing heat flux, there is a gradual predominance of boiling heat transfer over convection as the heat transfer mechanism. The pressure drop drastically increases with the vapor amount flowing into the system, regardless of the pin fin height; the boiling curves for the higher fin height show a much smaller slope and a smaller wall superheat than the fin with the smallest height, and consequently, a high heat transfer performance. For lower inlet subcooling temperature, a larger region of the heat sink is filled with vapor, degrading the heat transfer performance compared to higher inlet subcooling temperature.*

Keywords: *convective boiling, HFE-7100, pin fin geometry, pressure drop, heat transfer coefficient*

1. INTRODUCTION

An alternative to modifying the configuration of microchannels to minimize the instabilities present in this system is using segmented or micro-finned microchannels (micro pin fins). The recent development of microfabrication

techniques has allowed complex geometries on a reduced scale; thus, in recent years, several studies involving heat transfer in micro pin-fins heat sinks have been carried out in order to characterize the heat transfer mechanisms and to predict the thermal and fluid dynamic behavior of these systems. The micro fins can have different shapes and sizes and be arranged in different patterns to improve heat transfer (Tullius, 2012; Liang and Mudawar, 2019; Li et al., 2020). It is also noteworthy that the ideal spacing of the fins depends on the working fluid and its subcooling in the system. The mini and micro-finned channel arrangements are considered a promising structure for compact heat sinks (McNeil et al., 2014).

Deng et al. (2019) proposed a new type of heat sink with pin fin-interconnected reentrant microchannels (PFIRM) and tested it in convective boiling using water and ethanol as working fluids. Tests were performed under different subcooling conditions (40 and 10 °C) and mass fluxes (from 125 to 300 kg/m²s). An increase of 39-284% was observed in the heat transfer coefficient (HTC) for water and 29-220% for ethanol compared to parallel microchannels. Authors attributed this enhancement to the interconnected microchannels, which provide different paths for the vapor bubbles reducing the confinement effect. In addition, the interconnected spaces provided ideal conditions for the nucleation of vapor bubbles, contributing to the heat transfer improvement for the PFIRM. For pressure drop, Deng et al. (2019) reported an increase with increasing heat flux and vapor quality; moreover, the mass flux strongly influenced pressure drop at moderated and high heat fluxes.

Recently, Asrar et al. (2021) conducted an experimental investigation of convective boiling using R245fa in micro gaps improved with micro fins made of silicon (cylindrical pin fins with 150 μm in height and 200 μm of inter-fin space, in a staggered arrangement). Different conditions of mass flux (between 781 and 5210 kg/m²s) and inlet temperature (between 13 and 18 °C) were tested. The authors reported that HTC increased with increasing mass flux for the single-phase flow regime. For the two-phase flow regime, they compared the results with their previous works (Asrar et al., 2018); the new device showed better thermal performance than the previous one. Regarding pressure drop and vapor quality, Asrar et al. (2021) found the same behavior as Woodcock et al. (2015) and Chien et al. (2020), in which these parameters were independent of the heat flux in the single-phase regime but increased remarkably with the intensification of convective boiling.

The scientific community has extensively studied the heat transfer in segmented microchannels (or micro pin fins heat sinks), but there are still some knowledge gaps, with many of the works developed based on the trial and error method. Such studies take into account different dimensions and configurations of micro pin fins to understand the physical mechanisms responsible for heat transfer enhancement in an attempt to develop models to be applied on an industrial scale capable of predicting the heat transfer coefficient, the behavior of the critical heat flux and the pressure drop. Moreover, most studies utilizing micro pin fins used water as the working fluid owing to its wide availability and superior thermophysical properties; however, water is not suitable in embedded cooling solutions due to its high electrical conductivity (Jung et al., 2021).

Therefore, the current work investigates the thermal performance and pressure loss of HFE-7100 in micro pin fin heat sinks with different heights and their influence on pressure drop and heat transfer behavior. The geometrical and operating conditions were experimentally and computationally examined. Computational modeling was used to validate the thermal performance and pressure drop determined from the experiments for single-phase flow. The current study contributes to a better comprehension of heat removal capability, factors impacting heat transfer performance, and mechanisms responsible for heat transfer enhancement in such compact heat exchangers.

2. MATERIALS AND METHODS

2.1 Experimental apparatus

Figure 1 shows the experimental apparatus used in the present study. The working fluid is pumped from a reservoir to the flow loop; the HFE-7100 flow rate is set by a Coriolis mass flow meter (Yokogawa ROTAMASS Total Insight with 0.2 % mass flow accuracy) installed just upstream of the preheater (consisting of a horizontal copper tube heated by an electrical tape resistance). There is a bypass line used for the test facility maintenance. The pressure drop between inlet and outlet plenums is measured by two pressure transducers (OMEGA PX309 model, with 0.25% accuracy). The flow temperature is measured using previously calibrated K-type thermocouples (uncertainty of 0.3 °C) in the inlet and outlet plenums (both in contact with the fluid). The working fluid was cooled by a condenser and then returned to the reservoir.

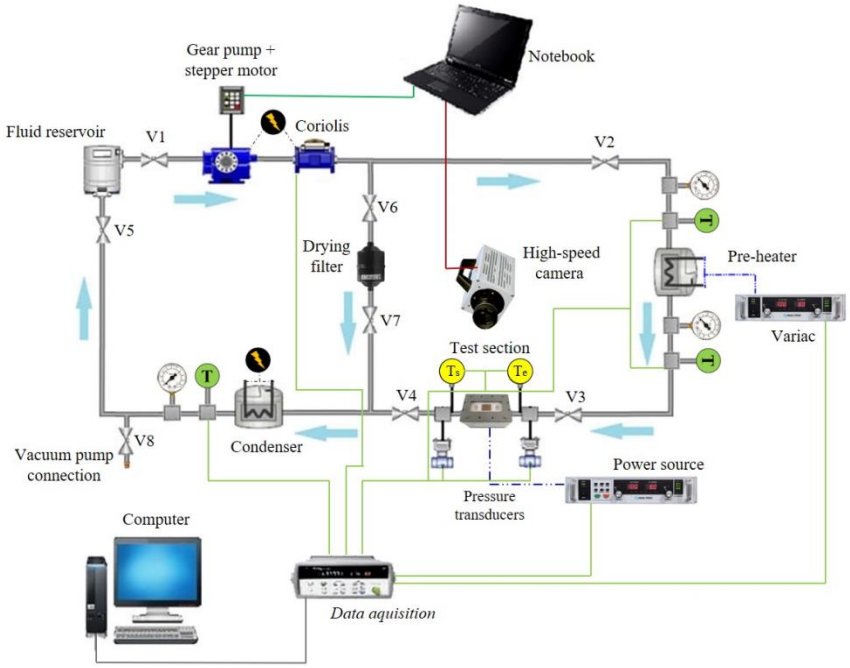

Figure 1. Schematic diagram of the experimental apparatus.

The heat sink (Figure 2) consists of a copper block with a 20 x 15 mm footprint with 972 micro-pin fins. The square micro pin fins (300 µm in width and 250 µm of inter-fin space) were manufactured using a CNC precision milling machine. In an aligned array, different heights (H) of micro pin fins – 160 µm named S1 and 350 µm named S2 – were tested.

Figure 2a shows that five holes (1 mm diameter) were drilled in the copper block for K-type thermocouples (A) to measure the wall temperature and verify the condition of 1-D heat conduction. An electrical resistance (cartridge type), embedded in the copper block (B) and controlled by a DC power supply, provides the heat flux.

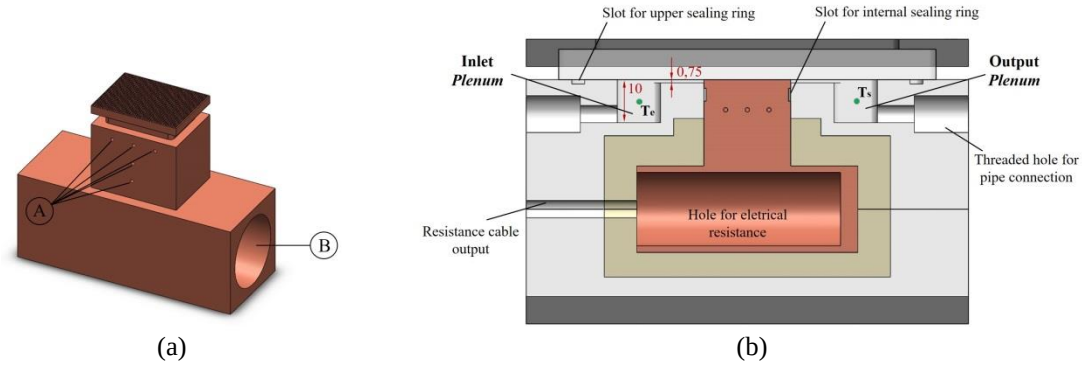

(a) (b)

Figure 2. Design of the micro pin fin heat sink. (a) Isometric view; (b) Front view with details; measurements in [mm].

As shown in Figure 2b, the thermal insulation is made with ceramic and polytetrafluoroethylene (PTFE); the working fluid is not heated before contacting the micro pin fins since the inlet and outlet plenums were machined on the PTFE. Two K-type thermocouples, one in the inlet and another in the outlet, measure the working fluid temperature (T_e and T_s, respectively). Flow homogenization channels were manufactured between the plenums and the heat sink to minimize flow entrance turbulence. Flow visualization (high-speed camera Photron SA3 model with 1000 fps and 1024 x 1024 resolution) is allowed by a polycarbonate plate (8 mm thick) covering the heat sink.

The geometric characterization of the micro pin fin heat sinks was performed by Zeiss® SteREO DiscoveryV8 and SEM EVO LS15 Zeiss® (Table 1).

Table 1. Structural characterization of the micro pin fin heat sinks.

Surface	STEREO		SEM (100x)
	Top view	Side view	
S1 H = 160 µm	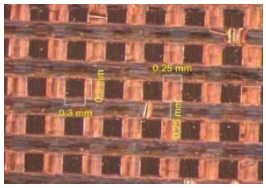	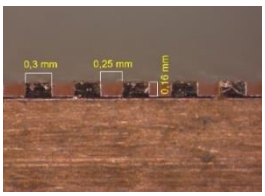	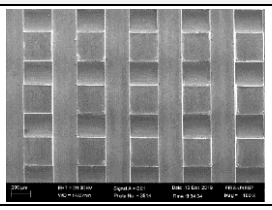
S2 H = 350 µm	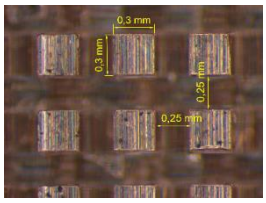	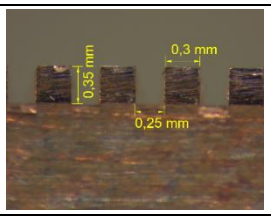	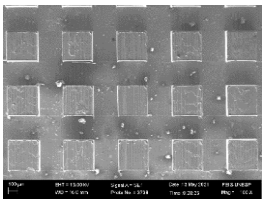

The experimental uncertainty was calculated using the free package developed in Python, called Uncertainties (© 2010-2016, EOL), based on the Taylor series method and standardized by the Bureau International des Poids et Mesures (BIPM). Consequently, for all tests carried out in the current study, the uncertainty of the heat flux, the heat transfer coefficient, and pressure drop varied from 4 to 16%, 7 to 21%, and 3 to 9%, respectively. It is worth mentioning that all analyses take into account the effective heat flux of the heater to the micro pin fin array, which is determined by subtracting heat loss to the surroundings from the power input; in the current study, the heat losses are less than 22% for all tests performed.

2.2 Experimental procedure

The consistency analysis aims to verify the coherence of the results obtained experimentally; thus, the results for the single-phase flow regime were compared to those obtained from a numerical analysis considering the same conditions. The simulation was based on the mass, momentum, and energy conservation equations with the second-order upwind scheme for energy and pressure and first-order for the momentum. The fluid flow was assumed steady-state, incompressible and laminar, and it was solved by adopting the Finite-Volume Method implemented in ANSYS Fluent 2020 R2. Figure 3 shows a schematic of the computational domain with appropriate boundary conditions. As a reference pressure, atmospheric pressure was defined; by considering the characteristics of a low-pressure system, the outlet pressure was set up as zero. No-slip condition was considered on the surfaces. Inlet mass flux and dimensions of the micro pin fins were from the experimental approach. The heat flux was distributed through the micro pin fins except for the top side (a polycarbonate piece thermally insulated the heat sink); for the inlet and outlet plenums, adiabatic wall conditions were considered.

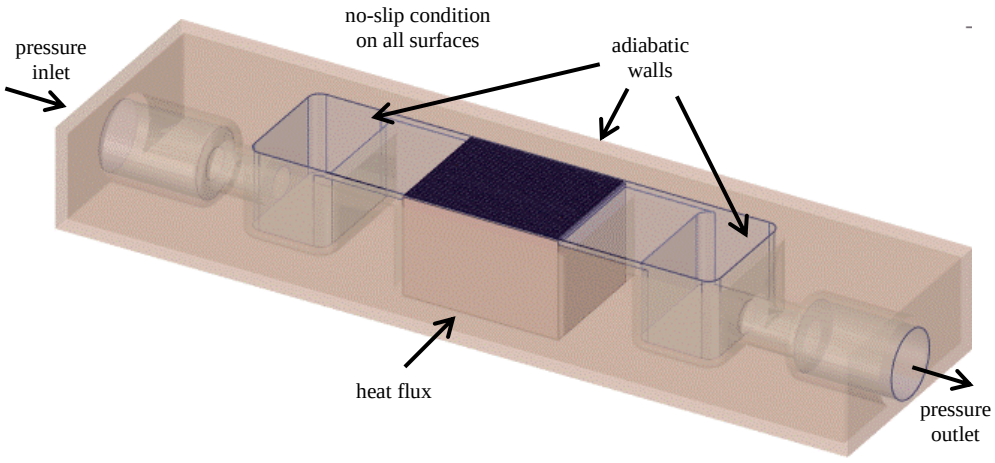

Figure 3. Computational domain of the heat sink with main boundary conditions.

The convergence occurred for meshes with 511.09k elements; the finer mesh was achieved when residuals were less than 10^{-5} for continuity equation and 10^{-6} for momentum and energy equations. The simulations used the segregated algorithm with SIMPLE algorithm for pressure-velocity coupling.

The mean absolute error ($MAE = \frac{1}{N}\sum_1^N \frac{|\phi_{exp}-\phi_{pred}|}{\phi_{exp}} \times 100\%$) of the total pressure drop and heater temperature were 7.1% and 5.6%, respectively. The computational results were consistent with the experimental data for the heat transfer coefficient; for both S1 e S2, the MAE was 5%. Therefore, the mean absolute errors of the experimental and simulation data for pressure drop and heat transfer coefficient are within the experimental uncertainty range.

After the validation, two-phase flow tests were performed for two different subcooling values, 10 ºC and 20 ºC; mass fluxes of 1000 and 1200 kg/m²s; and for different footprint heat fluxes from 10 kW/m² to the system limit, characterized by intense instability in the flow (reverse flow). The gear pump's rotation was set to achieve the desired mass flux; the preheater was adjusted until its outlet temperature was equal to the desired subcooling. A data acquisition system (Agilent 34970A) recorded the data every 2 seconds after the system achieved the steady-state regime, characterized by temperature variations lower than the thermocouples uncertainties (± 0.3 °C). The pressure, temperatures, mass flux, and electrical voltage are constantly monitored. Flow visualization was carried out using a high-speed camera. The same procedure is adopted during all the experimental tests to ensure repeatability.

3. RESULTS AND DISCUSSION

3.1 Effect of the inlet subcooling temperature

Figure 4 shows the effect of different inlet subcooling temperatures (10 and 20 ºC) on the flow boiling heat transfer for both surfaces (S1 e S2). The subcooling increase shifted the boiling curve to the left regardless of micro pin fin height. The HTC continuously increased with heat flux for all mass fluxes values and higher inlet subcooling temperature, while the HTC slightly decreased with high heat fluxes for lower inlet subcooling temperature. According to Yin *et al*. (2020a), such HTC behavior is due to the flow pattern transition into a confined annular flow, where partial dryout occurs on the surface as heat flux increases, leading to an increase in the surface temperature (being more pronounced for S1).

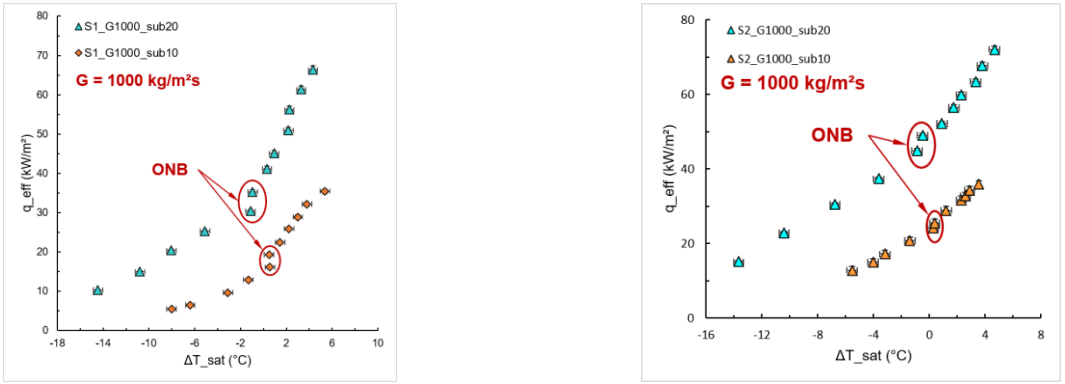

(a)

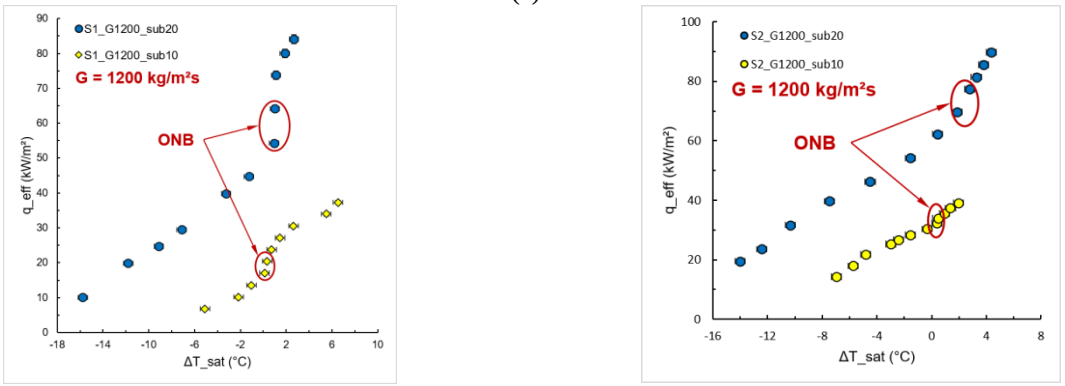

(b)

Figure 4. Effect of inlet subcooling temperature on flow boiling heat transfer of HFE-7100 for S1 and S2. (a) G = 1000 kg/m²s; (b) G = 1200 kg/m²s.

Analyzing the boiling curves of samples S1 and S2 is possible to observe the beginning of the nucleate boiling regime, indicated in Figure 4 as ONB (Onset Nucleate Boiling), and characterized by the sudden change in the slope of the boiling curve, reducing the surface temperature.

Figure 5 shows the effect of different inlet subcooling temperatures (10 and 20 ºC) on the pressure drop for both surfaces (S1 e S2). One can observe no significant effect of inlet subcooling temperatures on both surfaces' pressure drop in the single-phase flow region (for q'' < 30 kW/m^2). However, for the two-phase flow region, the pressure drop became larger as the inlet subcooling temperature decreased, regardless of the mass flux and micro pin fin height; a lower inlet subcooling temperature leads to a higher vapor quality through the heat sink, which increases the pressure drop.

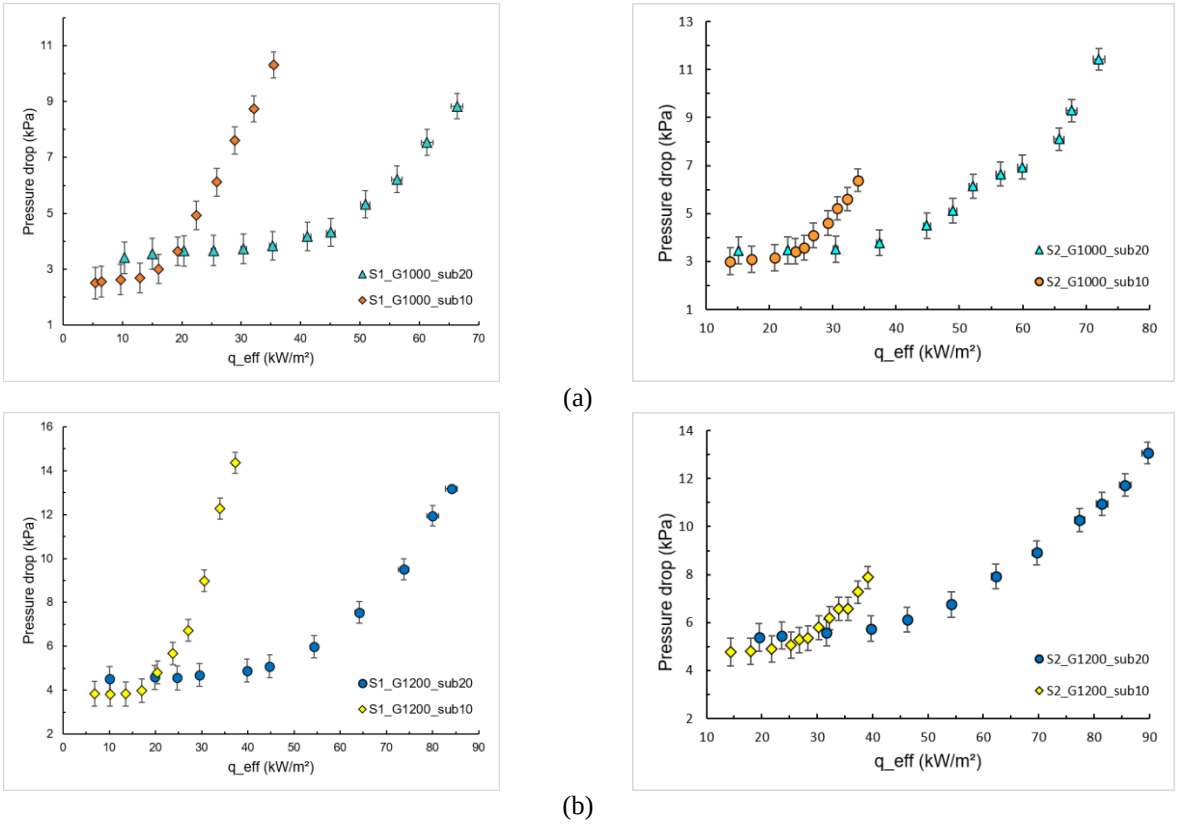

Figure 5. Effect of inlet subcooling on the pressure drop for S1 and S2. (a) G = 1000 kg/m²s; (b) G = 1200 kg/m²s.

3.2 Effect of the mass flux

Figure 6 shows the effect of different mass fluxes on the boiling curves, for S1 and S2, with different subcooling temperatures at the inlet of the heat sink. The influence of mass flux, G, on the convective flow boiling heat transfer was negligible for the inlet subcooling of 10 °C and the lowest micro pin fin height (S1); on the contrary, for the highest fin height, the fluid has more space to flow between the fins and more prominent is the convective effects (mass flux influence) in the single-phase flow region.

For the inlet subcooling of 20 ºC, an increase in the mass flux shifted the curves to the left, characterized by an HTC enhancement. Cheng and Wu (2021) indicated a gradual predominance of boiling heat transfer over convection as heat flux increases; furthermore, the micro-pin fins induced flow turbulence and strengthened convection heat transfer, the main heat dissipation component in subcooled convective boiling (Yin et al., 2020b).

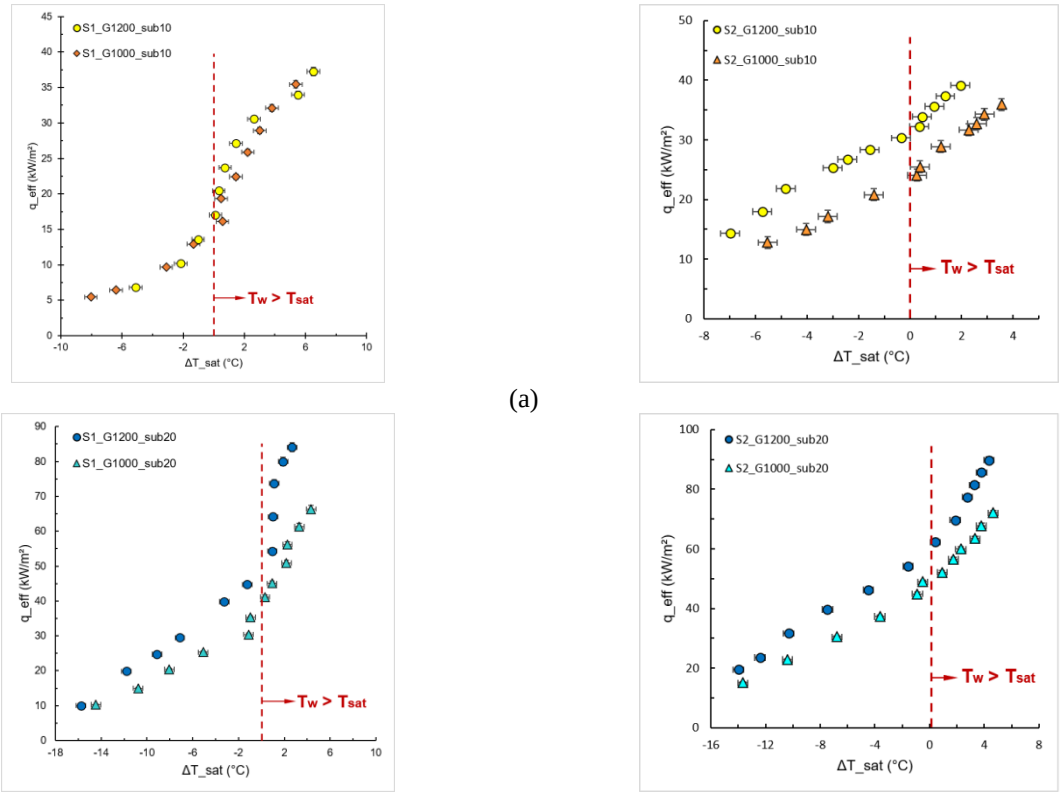

Figure 6. Effect of mass flux on flow boiling heat transfer of HFE-7100. (a) ΔT_{sub} = 10 ºC; (b) ΔT_{sub} = 20 ºC.

For both S1 and S2, increasing the mass flux increases the pressure drop for low heat flux values (single-phase flow region); however, no significant influence of mass flux on pressure drop was observed in the single-phase flow region for both inlet subcooling temperatures (10 and 20 ºC). As the heat flux increased (two-phase flow region), the pressure drop became more pronounced due to the increase in the vapor mass flowing through the heat sink; thus, the pressure drop is more influenced by the void fraction than by mass flux.

3.3 Effect of fin height

Figure 7 shows the effect of pin fin height on the boiling curves for different mass fluxes and inlet subcooling temperature of 10 °C. Considering the effective heat exchange area, we can infer that the increase in the effective area leads to an increase in the HTC, characterized by the shift of the boiling curve to the left. The same was reported by Kiyomura et al. (2020), who evaluated different configurations of micro fin surfaces during pool boiling of the HFE-7100. One can observe in Figure 7 that S2 presents a better HTC since its effective heat exchange area is approximately 55% greater than S1.

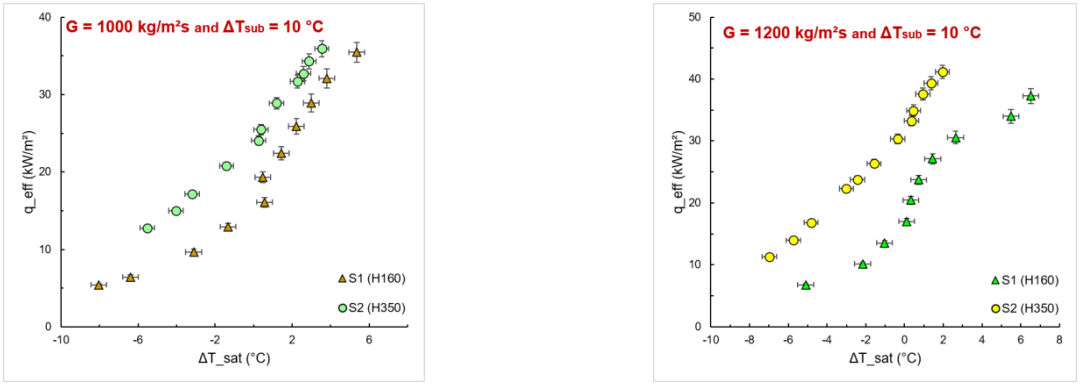

Figure 7. Effect of pin fin height on flow boiling heat transfer of HFE-7100 for ΔT_{sub} = 10 ºC. (a) G = 1000 kg/m²s; (b) G = 1200 kg/m²s.

3.4 Flow visualization

Figure 8 presents the boiling curve for S1 with G = 1200 kg/m²s and subcooling of 20 °C, with the respective visualization points. It is worth mentioning that similar behavior was observed for all test conditions. Flow boiling videos under these conditions can be found in the Supplementary Material.

Initially, the single-phase flow regime is predominant at lower heat flux, with no vapor bubbles (point (a), Figure 8). By increasing heat flux, isolated vapor bubbles nucleate preferentially between the adjacent fins, even though the working fluid temperature is lower than the saturation temperature - subcooled boiling condition (point (b), Figure 8). In the nucleate boiling region, after the ONB, nucleation sites are activated over the entire heating surface (point (c), Figure 8), increasing the departure frequency and the coalescence of vapor bubbles near the heat sink outlet. For high heat fluxes, the vapor core fills the entire length of the heat sink (point (d), Figure 8); the annular flow regime becomes more pronounced. A high void fraction is observed at the outlet of the heat sink, promoting thermal instabilities, a high-pressure drop, and the occurrence of reverse flow mainly observed for lower inlet subcooling temperature (reverse flow visualization link).

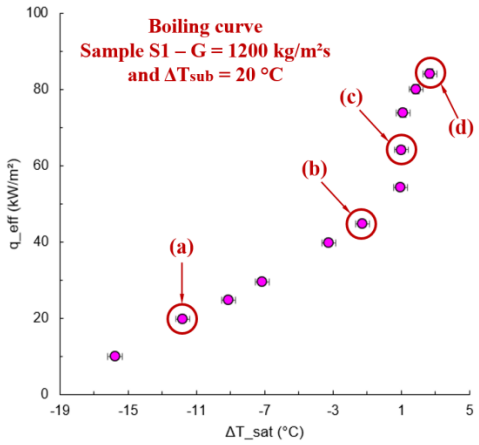

Figure 8. Boiling curve and high-speed camera images for S1. G = 1200 kg/m²s and ΔT_{sub} = 20 °C.

4. CONCLUSIONS

The current work studied the thermal and fluid dynamic behavior of convective boiling using HFE-7100 as working fluid in a heat sink based on square micro pin fins. Different micro pin fins were tested (heights of 160 and 350 µm in an aligned array) at different mass fluxes (1000 and 1200 kg/m²s) and two levels of inlet subcooling temperatures (10 and 20 °C). The boiling heat transfer and pressure drop behavior were evaluated for each test condition. The visualization of the experimental tests was performed using a high-speed camera to observe the transition from single-phase to two-phase flow and identify possible flow patterns and the occurrence of reverse flow. The main conclusions are summarized below:

- ✓ As the mass flux increases, HTC increases in the region where the effects of forced convection are dominant for each sample. However, when the effects of nucleate boiling overlap, the increase in mass flux does not guarantee a gain in HTC, especially for aligned arrays;
- ✓ The lower the inlet subcooling temperature, the lower the heat flux for the ONB occurrence, and a larger region of the heat sink is filled with vapor, which can promote the dryout incipience (decreasing the maximum heat flux);
- ✓ With a lower mass flux and inlet subcooling, the system becomes more sensitive to the effects of nucleate boiling, with significant gains in HTC due to the phase-change heat transfer (for S1 with G = 1000 kg/m²s and ΔT_{sub} = 10 °C, the HTC was increased about 39% compared to ΔT_{sub} = 20 °C for a heat flux of 30 kW/m^2). However, this can lead to the early dryout process;
- ✓ Pressure drop increases substantially with an increase of vapor amount flowing into the heat sink, which becomes more pronounced for lower subcooling, leading to the fluid dynamic limit of the system at lower heat fluxes compared to higher subcooling;
- ✓ An increase in the effective area leads to an increase in the HTC; thus, the taller the micro pin fins, the higher the heat exchange area, leading to an HTC enhancement;
- ✓ The reverse flow occurrence was observed more intensely for the lowest inlet subcooling temperature; the high vapor core acts as a barrier to the flow, degrading the HTC, increasing the pressure drop and causing thermal and fluid dynamic instabilities.

5. ACKNOWLEDGEMENTS

The authors are grateful for the financial support from the PPGEM – UNESP/FEIS, CAPES, CNPq (grant number 458702/2014-5 and 309848/2020-2), and FAPESP (grants numbers 2013/15431-7 and 2019/02566-8). The authors also extend their gratitude to Prof. Dr. Alessandro Roger Rodrigues from Escola de Engenharia de São Carlos/USP and Prof. Dr. Ricardo Arai from IFSP/São Carlos for their important contribution to this work.

6. REFERENCES

Asrar, P.; Ghiaasiaan, S. M.; Joshi, Y. K., 2021. "Two-Phase Heat Transfer and Flow Regimes in Pin Fin-Enhanced Microgaps – Effect of Pin Spacing". *Journal of Heat Transfer – ASME*, vol. 143, 023001-1.

Asrar, P.; Zhang, X.; Green, C. E.; Bakir, M.; Joshi, Y. K., 2018. "Flow boiling of R245fa in a microgap with staggered circular cylindrical pin fins". *International Journal of Heat and Mass Transfer*, vol. 121, p. 329-342.

Cheng, X., Wu, H., 2021. "Improved flow boiling performance in high-aspect-ratio interconnected microchannels". *International Journal of Heat and Mass Transfer*, Vol. 165, p. 120627.

Chien, L.H.; Cheng, Y.T.; Lai, Y.L.; Yan, W.M.; Ghalambaz, M. Experimental and numerical study on convective boiling in a staggered array of micro pin-fin microgap. *International Journal of Heat and Mass Transfer*, vol. 149. 119203, 2020.

Deng, D.; Chen, L.; Wan, W.; Fu, T.; Huang, X., 2019. "Flow boiling performance in pin fin-interconnected reentrant microchannels heat sink in different operational conditions". *Applied Thermal Engineering*, vol. 150, p. 1260-1272.

Jung, D., Lee, H., Kong, D., Cho, E., Jung, K. W., Kharangate, C. R., ... & Lee, H., 2021. "Thermal design and management of micro-pin fin heat sinks for energy-efficient three-dimensional stacked integrated circuits". *International Journal of Heat and Mass Transfer*, 175, 121192.

Kiyomura, I. S., Nunes, J. M., de Souza, R. R., Gajghate, S. S., Bhaumik, S., Cardoso, E. M., 2020. "Effect of microfin surfaces on boiling heat transfer using HFE-7100 as working fluid". *Journal of the Brazilian Society of Mechanical Sciences and Engineering*, *42*(7), 1-13.

Li, W.; Dai, R.; Zeng, M.; Wang, Q., 2020. "Review of two types of surface modification on pool boiling enhancement: passive and active". *Renewable and Sustainable Energy Reviews*, v. 130, p. 109926.

Liang, G.; Mudawar, I., 2019. "Review of pool boiling enhancement by surface modification". *International Journal of Heat and Mass Transfer*, v. 128, p. 892-933.

McNeil, D. A.; Raeisi, A. H.; Kew, P. A.; Hamed, R. S., 2014. "An investigation into flow boiling heat transfer and pressure drop in a pin–finned heat sink". *International Journal of Multiphase Flow*, vol. 67, p. 65-84.

Tullius, J.; Tullius, T.; Bayazitoglu, Y., 2012. "Optimization of short micro pin fins in minichannels". *International Journal of Heat Mass Transfer*, vol. 55, p. 3921–3932.

Woodcock, C.; Yu, X.; Plawsky, J.; Peles, Y., 2015. "Piranha Pin Fin (PPF) - Advanced flow boiling microstructures with low surface tension dielectric fluids". *International Journal of Heat and Mass Transfer*, vol. 90, p. 591-604.

Yin, L., Chauhan, A., Recinella, A., Jia, L., Kandlikar, S.G., 2020a. "Subcooled flow boiling in an expanding microgap with a hybrid microstructured surface". *International Journal of Heat and Mass Transfer,* Vol. 151, p. 119379.

Yin, L., Jiang, P., Xu, R., Hu, H., 2020b. "Water flow boiling in a partially modified microgap with shortened micro pin fins". *International Journal of Heat and Mass Transfer,* Vol. 155, p. 119819.

7. RESPONSIBILITY NOTICE

The authors are the only ones responsible for the printed material included in this paper.